End-to-end deep learning and sensor fusion for non-invasive BP monitoring using multivariate physiological signals

Pietro Cerveri[1,2], Mattia Sarti[1], Matteo Rossi[1,2], Giulia Alessandrelli[1,2], Carolina Lombardi[2,3], Luca Mainardi[1]

[1] Department of Electronics, Information and Bioengineering, Politecnico di Milano, Milan, Italy
[2] Istituto Auxologico Italiano, Milan, Italy
[3] Università degli Studi di Milano Bicocca, Milan, Italy

Abstract

Cuffless estimation of arterial blood pressure (ABP) is an ongoing topic of research and development that may revolutionize home monitoring. Into this path, innovative artificial intelligence (AI) tools, especially deep neural networks based on end-to-end computation, have gained much attention as they can leverage the bundle of signals acquired by integrated wearable devices to estimate directly the ABP, avoiding the assessment of intermediate features. In this work, we performed a feasibility analysis testing different neural architectures to process in bundle ECG and PPG signals to estimate continuously the BP. Data were collected from an already processed version of the MIMIC-II dataset from physionet.org. The reconstructed ABP was only partially accurate (mean absolute error in the range of 10 mmHg) due to the questionable quality of the data, despite extensive noise and outliers removal. This poses questions about the role of end-to-end approaches that, while saving effort in feature-engineered detection, appears to be very sensitive to the input data quality.

1. Introduction

Cardiovascular diseases (CVD) represent one of the dominant cause of death including a vast majority of complications with large impact on human health, such as myocardial infarction and stroke and their incidence is determined by a large multitude of factors [1]. Among these, high blood pressure (BP), unless addressed in its early stages, may develop into chronic hypertension and contribute to the increase of CVD risk [2]. BP measurement on a long-term basis has been identified as the main technique to detect hypertensive conditions [3]. The measure of BP is traditionally performed by ambulatory blood pressure monitoring (ABPM), requiring an arm-cuff device called pressure Holter and harnessing the oscillometric technique, with long-term measurements typically executed on a 24-48 hrs basis at intervals of 15-30 minutes. However, some specific events, such as masked hypertension and white coat phenomenon, make intermittent measurements inconclusive requiring continuous recording to ensure the clinical assessment of hypertensive conditions [4]. Likewise, being invasive and substantially uncomfortable, ABPM may interfere with sleep quality because of the device cuff inflation and frequency of measurements, with the occurrence of further confounding variability. Less invasive monitoring approaches avoids the cuff exploiting volume clamp, coupled to finger photopletismography, and tonometry applanation. Both techniques however demand active mechanical stimulation limiting again the use in daily life activities and during overnight [5]. Non-invasive BP monitoring has recently received a major boost with the introduction of wearable devices capable of unobstructively measuring electrocardiographic (ECG), photopletismographic (PPG) and phonocardiagraphic (PCG) signals [6]. They make use of intermediate physiological quantities such as the R-wave peak and cardiac sounds, detected in ECG and PCG respectively, and specific PPG fiducial points to compute transit time of the blood pulse (PTT) at a peripheral site. The first cardiac sound (S1), occurring at the beginning of ventricular systole and corresponding to the mitral and tricuspid (atrioventricular) valve closure, has been proposed in substitution of the R-wave peak as proximal timing for PTT estimation to avoid pre-ejection period (PEP) [7]. For the distal timing, fiducial points as the foot, the maximum slope and the systolic peak, detected in the PPG waveform in the same cardiac cycle of the selected proximal event, may be used [8]. Models relating BP to PTT have been extensively studied spanning non-linear regression, like inverse model [9–11], and analytical functions, like the Moens-Korteweg (M-K) model [12, 13], respectively. In this regards, the automatic and accurate identification of events and fiducial points in the signals becomes fundamental to guarantee a reliable

estimate of the PTT. In order to overcome issues related to accurate identification of fiducials, more recently research interest has been focused on end-to-end computation of the BP leveraging the bundle of signals acquired by integrated wearable devices and deep learning techniques [14–16]. In this work we performed a feasibility analysis testing different architectures of deep neural networks to process in bundle ECG and PPG signals to estimate continuously the BP. Data were collected from a publicly available dataset.

2. Methods

2.1. Dataset

The dataset used in this work, freely available from [17], was originally collected from MIMIC II (Multiparameter Intelligent Monitoring in Intensive Care II) database (physionet.org). MIMIC II contains physiologic signals and vital signs time series captured from patient monitors, and comprehensive clinical data obtained from hospital medical information systems, for tens of thousands of Intensive Care Unit (ICU) patients. Data were collected between 2001 and 2008 from a variety of ICUs (medical, surgical, coronary care, and neonatal) in a single tertiary teaching hospital. The available data underwent noise removal and outlier cleaning. The dataset, incorporating electrocardiogram (ECG), photoplethysmograph (PPG), and arterial blood pressure (ABP) signals (Fig. 1), consisted of a cell array of matrices, each cell is one record part. In each matrix, each row corresponds to one signal channel as: 1) PPG signal, FS=125Hz; photoplethysmogram from fingertip; 2) ECG signal, FS=125Hz; electrocardiogram from channel II; 3) ABP signal, FS=125Hz; invasive arterial blood pressure (mmHg). We performed a systematic in-depth analysis to validate signal quality, which revealed residual systematic noise and artifacts, despite pathological variability, of relevant entity. Waveform distortions, signal interruption, wrong ECG channel and both low frequency and high frequency noise were detected (Fig. 2). In order to reduce potential negative effect on the envisaged ABP estimation, an additional preprocessing step, despite the dataset was given as already preprocessed, was put in place to mainly filter out false II lead ECG signals and completely useless PPG and ABP signals. As far as ECG is concerned, the maximum of normalized cross-correlation with a representative kernel of a reliable ECG waveform was used to exclude useless ECG records. Likewise, PPG signals were cross-checked against a representative kernel and corresponding records excluded in cases the normalized cross-correlation were lower than a predefined threshold. Further, according to the literature [18], records were retained for valid ABP signal according to heuristic DBP and SBP thresholds ($50 < \text{DBP} < 130$ mmHg, $80 < \text{SBP} < 180$ mmHg). Without lack of generality, the considered record was 7.68 s long, corresponding to 960 samples. This was the input size for all the implemented models. Out of 278825 original 960-sample long records exhibiting a correct ECG lead shape, 65102 were used in the training and testing phase.

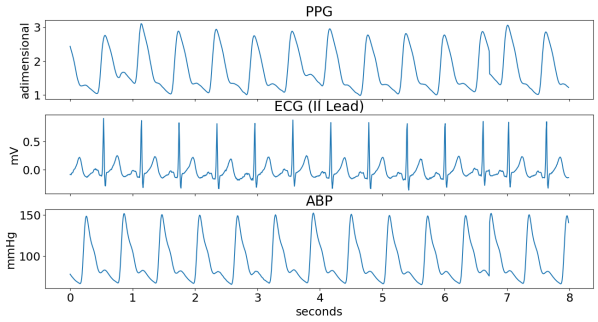

Figure 1. Example of an 8 s record featuring good quality of the three signals.

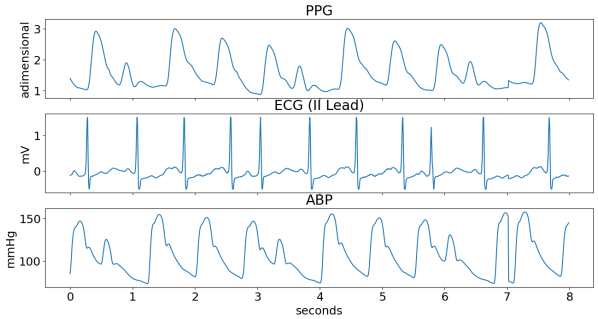

Figure 2. Example of an 8 s record featuring low quality of the three signals with artifacts that distort the waveforms.

2.2. Deep networks and metrics

Three main neural architectures, featuring the same output, namely the ABP temporal signal, were defined according to the specific encoding of the input as: 1) a fully-convolutional 1D U-Net with inputs as stacked (PPG and ECG) signals represented in the time domain; 2) an encoder(fully-connected)-decoder(fully-convolutional) network created to work on input signals represented in the frequency domain as stack of Fourier Transform magnitude and phase vectors for both PPG and ECG signals; 3) a fully-convolutional 2D U-Net with 2D inputs represented in the time-frequency domain as PPG and ECG spectrograms stacked as different channels (Table 1). As far as the third architecture is concerned, the spectrogram was described in terms of frequency bins and time bins, for both signals. The performance of the ABP signal regression was reported as mean absolute error (MAE).

Table 1. Hyperparameters of the three architectures considered in this work. In the third architecture the input spectrograms were computed considering 33 frequency bins and 29 time bins.

Model	Input size	Output size	Weights
1D U-Net	(960, 2)	(960, 1)	46M
Enc/Dec	(960, 4)	(960, 1)	22M
2D U-Net	(33, 29, 2)	(960, 1)	17M

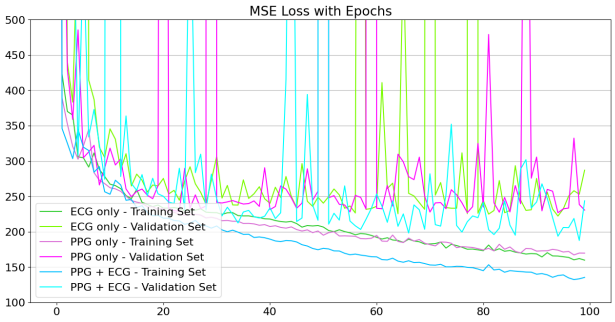

Figure 3. Mean squared error (MSE) on the training set and on the validation set with training epochs, for different setups. The setting where the input was ECG and PPG signal bundle performed better than the setting where the input was either ECG or PPG.

3. Results

The training was performed on a GeForce-GTX 1600 NVidia GPU and took about 12hrs using a batch size of 256 records. Heuristic tuning of the stop criterion led to identify about 100 epochs for quasi-optimal convergence. Model hyperparameters were tuned so as to minimize both under-fitting and over-fitting. Specific ablation analysis was performed on the first architecture to evaluate the role of signal bundle. As expected, the comparison between stacking PPG and ECG together and using only one signal at a time was in favour of the first strategy (Fig. 3). Interestingly, the networks trained with either ECG or PPG attained very similar results, $\sim$17% lower than the ECG-PPG input combination though. Loss and metrics on the validation set were nonetheless sensibly higher than those on the training set, this questioning about the generalization capabilities of the network. Accuracy results, across the three network models, allowed to highlight that model #1 (MAE: 9.87 mmHg) overcame the other two models (MAE: 17.20, 17.19) (Table 2). Two specific ABP reconstructions, obtained with network #1 featured high (MAE: 4.85 mmHg) and low (MAE: 9.21 mmHg) quality respectively (Figgs. 4 and 5), despite both PPG and ECG signals appeared of reasonable quality. Nonetheless, a closer look to ECG signal of the second case outlined distortion of the waveform following QRS interval.

Table 2. MAE results attained with the three architectures.

Model	MAE
#1	9.87 mmHg
#2	17.20 mmHg
#3	17.19 mmHg

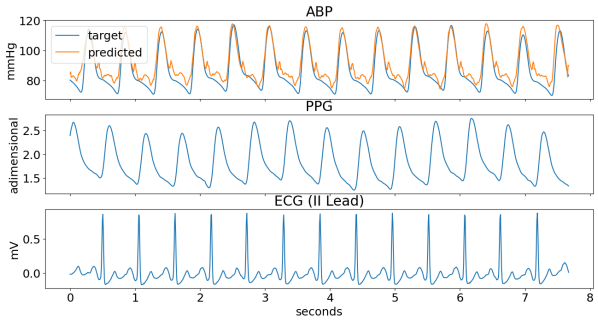

Figure 4. Reconstructed ABP signal with high accuracy (MAE: 4.85 mmHg).

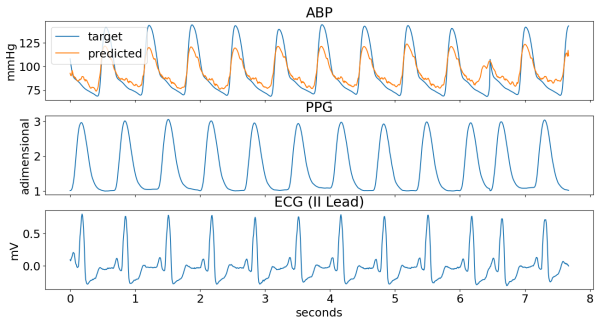

Figure 5. Reconstructed ABP signal with low accuracy (MAE: 9.21 mmHg).

4. Discussion

4.1. Findings

Results (cfr. Fig. 3) confirmed the benefit of incorporating PPG and ECG rather than considering the effects of the single signal. Quantitative results highlighted the poor accuracy when using frequency and spectrogram, this motivated likely by the underestimation of the network hyperparameters role, which might require additional tuning efforts. The first architecture provided results only partially in agreement with the results (SBP-MAE: 3.96 mmHg; DBP-MAE: 2.39 mmHg) of similar approaches (MIMIC-II dataset, mapping PPG to BP) in the literature [18]. Nonetheless our error was measured along all the waveform and not only taken at systole and diastole events, and the test was performed on 65102 records (62M samples

against 3M using in [18]).

4.2. Challenges, issues and conclusions

Recent interest in AI-based end-to-end approach for cuffless ABP estimation is motivated by two main reasons: 1) avoiding the detection of fiducials in physiological signals; 2) achieving the reconstruction of a complete continuous signal, rather that computing systolic and diastolic BP only. The initial analysis of the available dataset outlined the fundamental need of thorough and systematic revision of signal records in publicly available datasets as MIMIC-II even in case of prior pre-processing [17]. This also poses questions about the reliability of the comparisons of many algorithms in the literature making used of such datasets for network training and testing. In conclusion, we remark that the findings of this paper, while preliminary, indicate that ABP continuous estimation with end-to-end deep network is a recent and actively emerging area of research. Nonetheless, the clinical translation of such techniques still demands for extensive validation.

Acknowledgments

The work was supporeted by Italian MInistry of University and Research - PON Program Green and Innovation, 2021-2023.

References

[1] Muntner P, Shimbo D, Carey RM, Charleston JB, Gaillard T, Misra S, Myers MG, Ogedegbe G, Schwartz JE, Townsend RR, Urbina EM, Viera AJ, White WB, Jr JTW. Measurement of blood pressure in humans: A scientific statement from the american heart association. Hypertension 03 2019;.

[2] Pierdomenico SD, Pierdomenico AM, Cuccurullo F. Morning blood pressure surge, dipping, and risk of ischemic stroke in elderly patients treated for hypertension. American Journal of Hypertension 04 2014;27.

[3] Parati G, Stergiou G, O'Brien E, Asmar R, Beilin L, Bilo G, Clement D, Sierra A, de Leeuw P, Dolan E, Fagard R, Graves J, Head G, Imai Y, Kario K, Lurbe E, Mallion JM, Mancia G, Mengden T, Zhang Y. European society of hypertension practice guidelines for ambulatory blood pressure monitoring. Journal of Hypertension 05 2014;32:1359.

[4] Pickering T, Eguchi K, Kario K. Masked hypertension: A review. Hypertension research official journal of the Japanese Society of Hypertension 06 2007;30:479–88.

[5] Wax DB, Lin H, Leibowitz AB. Invasive and concomitant noninvasive intraoperative blood pressure monitoring. Anesthesiology 11 2011;115.

[6] Bote JM, Recas J, Hermida R. Evaluation of blood pressure estimation models based on pulse arrival time. Computers text Electrical Engineering 2020;84:106616. ISSN 0045-7906.

[7] Esmaili A, Kachuee M, Shabany M. Nonlinear cuffless blood pressure estimation of healthy subjects using pulse transit time and arrival time. IEEE Transactions on Instrumentation and Measurement 2017;66:3299–3308. ISSN 1557-9662.

[8] Ding XR, Zhang YT, Liu J, Dai WX, Tsang HK. Continuous cuffless blood pressure estimation using pulse transit time and photoplethysmogram intensity ratio. IEEE transactions on bio medical engineering May 2016;63:964–972. ISSN 1558-2531.

[9] Mukkamala R, Hahn JO, Inan OT, Mestha LK, Kim CS, Töreyin H, Kyal S. Toward ubiquitous blood pressure monitoring via pulse transit time: Theory and practice. IEEE transactions on bio medical engineering August 2015; 62:1879–1901. ISSN 1558-2531.

[10] Sharma M, Barbosa K, Ho V, Griggs D, Ghirmai T, Krishnan S, Hsiai T, Chiao JC, Cao H. Cuff-Less and Continuous Blood Pressure Monitoring: A Methodological Review. Technologies may 2017;5(2):21. ISSN 2227-7080.

[11] Lee J, Yang S, Lee S, Kim HC. Analysis of pulse arrival time as an indicator of blood pressure in a large surgical biosignal database: Recommendations for developing ubiquitous blood pressure monitoring methods. Journal of Clinical Medicine 2019;8(11). ISSN 2077-0383.

[12] Shahmirzadi D, Li RX, Konofagou EE. Pulse-wave propagation in straight-geometry vessels for stiffness estimation: theory, simulations, phantoms and in vitro findings. Journal of biomechanical engineering 2012;134(11):114502.

[13] Marzorati D, Bovio D, Salito C, Mainardi L, Cerveri P. Chest wearable apparatus for cuffless continuous blood pressure measurements based on ppg and pcg signals. IEEE Access 2020;8:55424–55437. ISSN 2169-3536.

[14] Li F, Tang H, Shang S, Mathiak K, Cong F. Classification of heart sounds using convolutional neural network. Applied Sciences 2020;10:3956. ISSN 2076-3417.

[15] Lee D, Kwon H, Son D, Eom H, Park C, Lim Y, Seo C, Park K. Beat-to-beat continuous blood pressure estimation using bidirectional long short-term memory network. Sensors 12 2021;21(96):96. ISSN 1424-8220.

[16] Barvik D, Cerny M, Penhaker M, Noury N. Noninvasive continuous blood pressure estimation from pulse transit time: A review of the calibration models. IEEE Reviews in Biomedical Engineering 2022;15:138–151. ISSN 1941-1189.

[17] Kachuee M, Kiani MM, Mohammadzade H, Shabany M. Cuffless blood pressure estimation algorithms for continuous health-care monitoring. IEEE transactions on bio medical engineering April 2017;64:859–869. ISSN 1558-2531.

[18] Li Z, He W. A continuous blood pressure estimation method using photoplethysmography by grnn-based model. Sensors 10 2021;21(7207):7207. ISSN 1424-8220.

Address for correspondence:

Pietro Cerveri
via Ponzio 34/5 20133 Milan, Italy
pietro.cerveri@polimi.it